



ELSEVIER

Available online at [www.sciencedirect.com](http://www.sciencedirect.com)

SCIENCE @ DIRECT®

Thin-Walled Structures 42 (2004) 701–717

THIN-WALLED  
STRUCTURES

[www.elsevier.com/locate/tws](http://www.elsevier.com/locate/tws)

# A semi-analytical model for global buckling and postbuckling analysis of stiffened panels

Eirik Byklum<sup>a,\*</sup>, Eivind Steen<sup>a</sup>, Jørgen Amdahl<sup>b</sup>

<sup>a</sup> *Det Norske Veritas, Maritime Technology and Production Centre, Veritasveien 1, N-1322 Høvik, Norway*

<sup>b</sup> *Department of Marine Structures, Norwegian University of Science and Technology, N-7491 Trondheim, Norway*

Received 27 February 2003; received in revised form 24 November 2003; accepted 23 December 2003

---

## Abstract

A computational model for global buckling and postbuckling analysis of stiffened panels is derived. The loads considered are biaxial in-plane compression or tension, shear, and lateral pressure. Deflections are assumed in the form of trigonometric function series, and the principle of stationary potential energy is used for deriving the equilibrium equations. Lateral pressure is accounted for by taking the deflection as a combination of a clamped and a simply supported deflection mode. The global buckling model is based on Marguerre's non-linear plate theory, by deriving a set of anisotropic stiffness coefficients to account for the plate stiffening. Local buckling is treated in a separate local model developed previously. The anisotropic stiffness coefficients used in the global model are derived from the local analysis. Together, the two models provide a tool for buckling assessment of stiffened panels. Implemented in the computer code PULS, developed at Det Norske Veritas, local and global stresses are combined in an incremental procedure. Ultimate limit state estimates for design are obtained by calculating the stresses at certain critical points, and using the onset of yielding due to membrane stress as the limiting criterion.

© 2004 Elsevier Ltd. All rights reserved.

*Keywords:* Stiffened panel; Global deflection; Buckling; Postbuckling; Ultimate strength; Analytical model; Energy principles

---

---

\* Corresponding author. Tel.: +47-67-57-99-00; fax: +47-67-57-99-11.  
E-mail address: [eirik.byklum@dnv.com](mailto:eirik.byklum@dnv.com) (E. Byklum).

## 1. Introduction

The global capacity of ships and offshore structures depends to a large extent on the buckling strength of the individual stiffened panels. In order to achieve safe and economical design, it is therefore necessary to have a tool for buckling assessment of stiffened panels. Such a tool should be computationally efficient and as accurate as possible. The global buckling model presented in the following is developed as one part of such a tool. Together with a local buckling model presented in [1], it may be used for buckling assessment of stiffened panels. The models are implemented in PULS, which is a computer code for buckling assessment developed at Det Norske Veritas. Local and global stresses are combined in an incremental procedure [2,3], and ultimate limit state estimates are obtained.

The stiffened panel is assumed to consist of a rectangular plate area with longitudinal stiffeners in one direction and heavy transverse girders in the other direction, as shown in Fig. 1. This is a typical configuration for the deck, side, or bottom of a ship hull girder. The loads acting on a stiffened panel in a ship are in-plane compression or tension, resulting from the overall hull girder bending moment or torsion, shear force resulting from the hull girder shear force, and lateral pressure resulting from internal cargo or the external sea.

The computational model for the global buckling is developed by considering the stiffened panel as a plate with anisotropic stiffness coefficients. The anisotropy is structural, meaning that it is caused by the plate stiffening. The material is assumed to be isotropic elastic. The local deformation of the plating and stiffeners is accounted for by applying a set of reduced anisotropic stiffness coefficients, which is derived from the local buckling model [1]. Due to the local buckling effects, the stiffness properties are reduced compared to the initial stiffness.

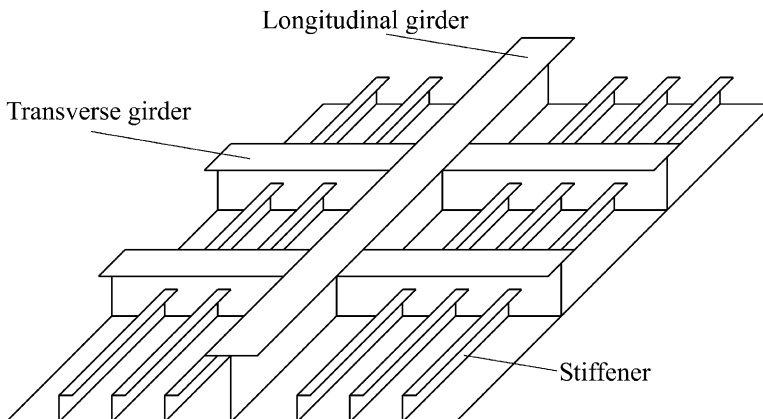


Fig. 1. Stiffened panel.

Consistent with the anisotropic/orthotropic plate theory, the global buckling mode involves lifting the stiffeners out-of-plane together with the plating, as illustrated in Fig. 2. With respect to the global and local mode interaction effect as implemented in the PULS code [2], the global deflections are assumed not to influence the local deformation, and the procedure may therefore be viewed upon as a kind of one-way interaction between local and global buckling.

The response of the stiffened plate during buckling is studied using the principle of stationary potential energy:

$$\delta\Pi = \delta U + \delta T = 0 \quad (1)$$

$\Pi$  is total potential energy,  $U$  is internal energy,  $T$  is the potential of the external loads, and  $\delta$  is the variational operator. Using trigonometric functions to represent the displacement, analytical expressions are found for the potential energy.

The stationary potential energy principle generates the nonlinear algebraic equilibrium equations, which are next solved numerically using perturbation methods [4]. The numerical procedure involves deriving the incremental stiffness matrices and load vectors, consistent with a first order perturbation expansion of the equilibrium equations. By stepping along the equilibrium path in very small increments, directly using the arc length parameter as control [5], equilibrium iterations are abandoned and fast and sufficiently accurate solutions are achieved. Numerical results confirming this are given in Section 5.

Previously, the large deflection response of unstiffened plates had been studied analytically by Ueda et al. [6] and Paik et al. [7]. In these studies, isotropic elastic plates were considered. The global deflection of a stiffened plate was studied analytically using a single degree of freedom model in [8]. The effect of local deformation was not accounted for. In the present work, the buckling and postbuckling problem is solved for plates with general anisotropic stiffness, and for a combination

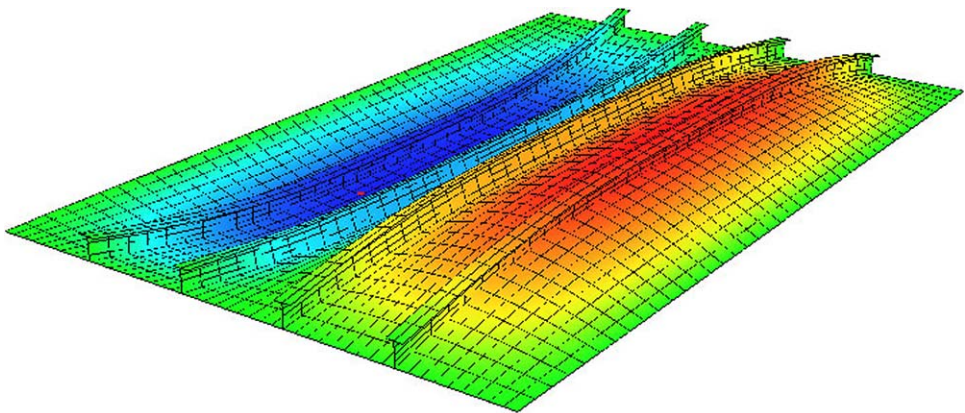


Fig. 2. Global buckling deflection in a stiffened panel.

of simply supported mode deflection and clamped mode deflection, using a two-span model philosophy (Fig. 5).

## 2. Definition of global stiffness coefficients

The global stiffness coefficients  $C_{ij}$  for the stiffened panel are defined as the change in load  $N_i$  resulting from a change in displacement  $\varepsilon_j$ , provided that all other displacements are kept fixed. The loads considered on the global level are defined as (see Fig. 3):

- $N_1$  axial force per unit breadth in  $x$ -direction
- $N_2$  axial force per unit length in  $y$ -direction
- $N_3$  shear flow
- $M_1$  resulting moment about the plate plane due to  $N_1$
- $M_2$  resulting moment about the plate plane due to  $N_2$
- $M_3$  torsional moment

The corresponding displacements are:

- $\varepsilon_1$  average strain in  $x$ -direction
- $\varepsilon_2$  average strain in  $y$ -direction
- $\varepsilon_3$  shear strain
- $\kappa_1$  curvature about the  $y$ -axis
- $\kappa_2$  curvature about the  $x$ -axis
- $\kappa_3$  torsion

It should be noted that these definitions are somewhat unusual, since  $N_3$  is shear flow rather than force in  $z$ -direction, and  $M_3$  is torsional moment rather than moment about the  $z$ -axis. The displacement parameters used are all average values. Hence, the stiffness coefficients may also be considered as averaged over the panel.

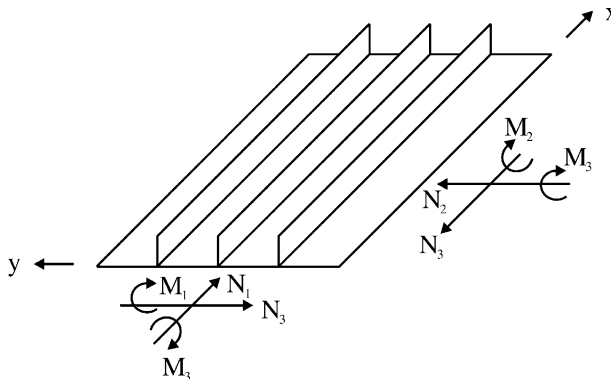


Fig. 3. Definition of global forces and moments.

Consistent with the first order perturbation expansion of the equilibrium solution, the incremental force–displacement relation for the stiffened panel is [9]:

$$\begin{bmatrix} \Delta N_1 \\ \Delta N_2 \\ \Delta N_3 \\ \Delta M_1 \\ \Delta M_2 \\ \Delta M_3 \end{bmatrix} = \begin{bmatrix} C_{11} & C_{12} & C_{13} & Q_{11} & Q_{12} & Q_{13} \\ C_{21} & C_{22} & C_{23} & Q_{21} & Q_{22} & Q_{23} \\ C_{31} & C_{32} & C_{33} & Q_{31} & Q_{32} & Q_{33} \\ Q_{11} & Q_{21} & Q_{31} & D_{11} & D_{12} & D_{13} \\ Q_{12} & Q_{22} & Q_{32} & D_{21} & D_{22} & D_{23} \\ Q_{13} & Q_{23} & Q_{33} & D_{31} & D_{32} & D_{33} \end{bmatrix} \begin{bmatrix} \Delta \varepsilon_1 \\ \Delta \varepsilon_2 \\ \Delta \varepsilon_3 \\ \Delta \kappa_1 \\ \Delta \kappa_2 \\ \Delta \kappa_3 \end{bmatrix} \tag{2}$$

The stiffness matrix is symmetric, so that  $C_{ij} = C_{ji}$  and  $D_{ij} = D_{ji}$ . The stiffness coefficients may be divided into a linear and a nonlinear part:

$$C_{ij} = C_{ij}^L + C_{ij}^{NL} \tag{3}$$

$$D_{ij} = D_{ij}^L + D_{ij}^{NL} \tag{4}$$

$$Q_{ij} = Q_{ij}^L + Q_{ij}^{NL} \tag{5}$$

The linear parts are the ones corresponding to classical orthotropic stiffness coefficients, and these are independent of load and displacement. The nonlinear parts are calculated using the local buckling model, and will be functions of load and displacement. For compressive loads they will be negative, resulting in a stiffness reduction.

### 3. Derivation of reduced stiffness

For calculation of the reduced stiffness coefficients to be used in the global buckling model, the total forces are written as follows:

$$\begin{bmatrix} \mathbf{N} \\ \mathbf{M} \end{bmatrix} = \begin{bmatrix} \mathbf{C} & \mathbf{Q} \\ \mathbf{Q}^T & \mathbf{D} \end{bmatrix}^L \begin{bmatrix} \varepsilon \\ \kappa \end{bmatrix} + \begin{bmatrix} \mathbf{g}_N(A_{mn}) \\ \mathbf{g}_M(A_{mn}) \end{bmatrix} \tag{6}$$

where  $\mathbf{g}_N(A_{mn})$  and  $\mathbf{g}_M(A_{mn})$  are nonlinear terms, which are due to local buckling effects. The reduced stiffness coefficients are then defined as:

$$C_{ij} = \frac{\partial N_i}{\partial \varepsilon_j} = C_{ij}^L + \frac{\partial g_{N_i}}{\partial \varepsilon_j} \tag{7}$$

$$Q_{ij} = \frac{\partial N_i}{\partial \kappa_j} = Q_{ij}^L + \frac{\partial g_{N_i}}{\partial \kappa_j} \tag{8}$$

$$= \frac{\partial M_j}{\partial \varepsilon_i} = Q_{ij}^L + \frac{\partial g_{M_j}}{\partial \varepsilon_i} \tag{9}$$

$$D_{ij} = \frac{\partial M_i}{\partial \kappa_j} = M_{ij}^L + \frac{\partial g_{M_i}}{\partial \kappa_j} \tag{10}$$

The reduced stiffness coefficients are derived using the local buckling model presented in [1]. First, the resultant forces and moments are calculated by integration

of the membrane stress:

$$N_i = \int_h \sigma_{ii} dz \quad (11)$$

$$M_i = \int_h z \sigma_{ii} dz \quad (12)$$

The neutral axis of the stiffener is not known, since it is continuously changing during buckling. The bending moment is therefore calculated about the middle plate plane. The neutral axis and the neutral bending stiffness coefficients can be calculated once the in-plane and bending stiffness are determined.

For open profile stiffeners, the following expressions were calculated in [1] for the internal axial and transverse force:

$$N_1 = E \frac{A_T}{b} \left[ 1 + \frac{v^2 bt}{A_T(1-v^2)} \right] \varepsilon_1 + \frac{vtE}{1-v^2} \varepsilon_2 + \frac{EA_s z_{gs}}{b} \kappa_1 + g_{N_1} \quad (13)$$

$$N_2 = \frac{vtE}{1-v^2} \varepsilon_1 + \frac{tE}{1-v^2} \varepsilon_2 + g_{N_2} \quad (14)$$

where  $A_T$  is the total cross-sectional area,  $A_s$  is the stiffener area, and  $z_{gs}$  is the distance from the plate plane to the centroid of the stiffener. The curvature  $\kappa_1$  is due to global deflection. The shear force and bending moment are:

$$N_3 = Gt\varepsilon_3 + g_{N_3} \quad (15)$$

$$M_1 = \frac{EA_s}{b} \varepsilon_1 + \frac{EI}{b} \kappa_1 + g_{M_1} \quad (16)$$

where  $I$  is the moment of inertia of the whole cross-section. The stiffness coefficients are found by differentiation of the above expressions. The linear parts are given directly as:

$$C_{11}^L = E \frac{A_T}{b} \left( 1 + \frac{v^2 bt}{A_T(1-v^2)} \right) \quad (17)$$

$$C_{12}^L = C_{21}^L = \frac{vtE}{1-v^2} \quad (18)$$

$$C_{22}^L = \frac{tE}{1-v^2} \varepsilon_2 \quad (19)$$

$$C_{33}^L = Gt \quad (20)$$

$$Q_{11}^L = \frac{EA_s z_{gs}}{b} \quad (21)$$

$$D_{11}^L = \frac{EI}{b} \quad (22)$$

All other linear coefficients are zero for open profile stiffeners. The nonlinear parts of the stiffness coefficients are calculated as:

$$C_{ij}^{\text{NL}} = \frac{\partial g_{N_i}}{\partial w_L} \frac{\partial w_L}{\partial \varepsilon_j} \quad (23)$$

$$Q_{ij}^{\text{NL}} = \frac{\partial g_{N_i}}{\partial w_L} \frac{\partial w_L}{\partial \kappa_j} \quad (24)$$

$$D_{ij}^{\text{NL}} = \frac{\partial g_{M_i}}{\partial w_L} \frac{\partial w_L}{\partial \kappa_j} \quad (25)$$

where  $w_L$  is the local deflection. The first part may be found directly by differentiation once  $\mathbf{g}_N$  and  $\mathbf{g}_M$  are known. They can be calculated from expressions for  $N_i$  and  $M_i$  derived for the local model in [1]. The second part is calculated using the equilibrium equations for the local buckling problem. By applying partial differentiation to the stationary potential energy, we get:

$$\frac{\partial(\partial\Pi/\partial w_L)}{\partial \varepsilon_i} = \frac{\partial^2\Pi}{\partial w_L^2} \frac{\partial w_L}{\partial \varepsilon_i} + \frac{\partial^2\Pi}{\partial w_L \partial \varepsilon_i} = \mathbf{0} \quad (26)$$

$$\frac{\partial(\partial\Pi/\partial w_L)}{\partial \kappa_1} = \frac{\partial^2\Pi}{\partial w_L^2} \frac{\partial w_L}{\partial \kappa_1} + \frac{\partial^2\Pi}{\partial w_L \partial \kappa_1} = \mathbf{0} \quad (27)$$

By introducing the incremental stiffness matrix  $\mathbf{K}$  and load vectors  $\mathbf{G}$ , defined as

$$\mathbf{K} = \frac{\partial^2\Pi}{\partial w_L^2} \quad (28)$$

$$\mathbf{G}_{\varepsilon_i} = \frac{\partial^2\Pi}{\partial w_L \partial \varepsilon_i} \quad (29)$$

$$\mathbf{G}_{\kappa_1} = \frac{\partial^2\Pi}{\partial w_L \partial \kappa_1} \quad (30)$$

we can write:

$$\mathbf{K} \frac{\partial w_L}{\partial \varepsilon_i} + \mathbf{G}_{\varepsilon_i} = \mathbf{0} \quad (31)$$

$$\mathbf{K} \frac{\partial w_L}{\partial \kappa_1} + \mathbf{G}_{\kappa_1} = \mathbf{0} \quad (32)$$

This means that

$$\frac{\partial w_L}{\partial \varepsilon_i} = -(\mathbf{K})^{-1} \mathbf{G}_{\varepsilon_i} \quad (33)$$

and

$$\frac{\partial w_L}{\partial \kappa_1} = -(\mathbf{K})^{-1} \mathbf{G}_{\kappa_1} \quad (34)$$

An example of how the stiffness coefficients may change during local deformation is given in Fig. 4. The calculations are for a steel angle bar (Table 1). The load is axial, and the imperfection is 1 mm in the local eigenmode.

The values plotted are the ratio between the nonlinear stiffness coefficients and the corresponding initial values.  $Q_{12}$  is divided by  $Q_{11}$  since  $Q_{12}^L$  is zero. The stiffness ratios are slightly smaller than 1.0 at the start of the analysis due to the imperfection. If the imperfection were larger, the stiffness ratios would also have smaller initial values.

It is seen that the stiffness reduction is significant for  $C_{11}$  and  $C_{22}$ , but the most drastic change is for  $C_{12}$ , which even changes sign. The reason is that  $C_{12}$  is positive for a flat plate due to the Poisson effect, while it becomes negative for large deflection due to membrane stretching. The change in  $Q_{11}$ ,  $Q_{12}$ , and  $D_{11}$  is small. There is some reduction in  $D_{n11}$ , which is the neutral bending stiffness. This coefficient is defined in the next section.

It is seen that the stiffness reduction is quite localized. The reduction occurs around the buckling strain, and the stiffness is almost constant after this. This is a

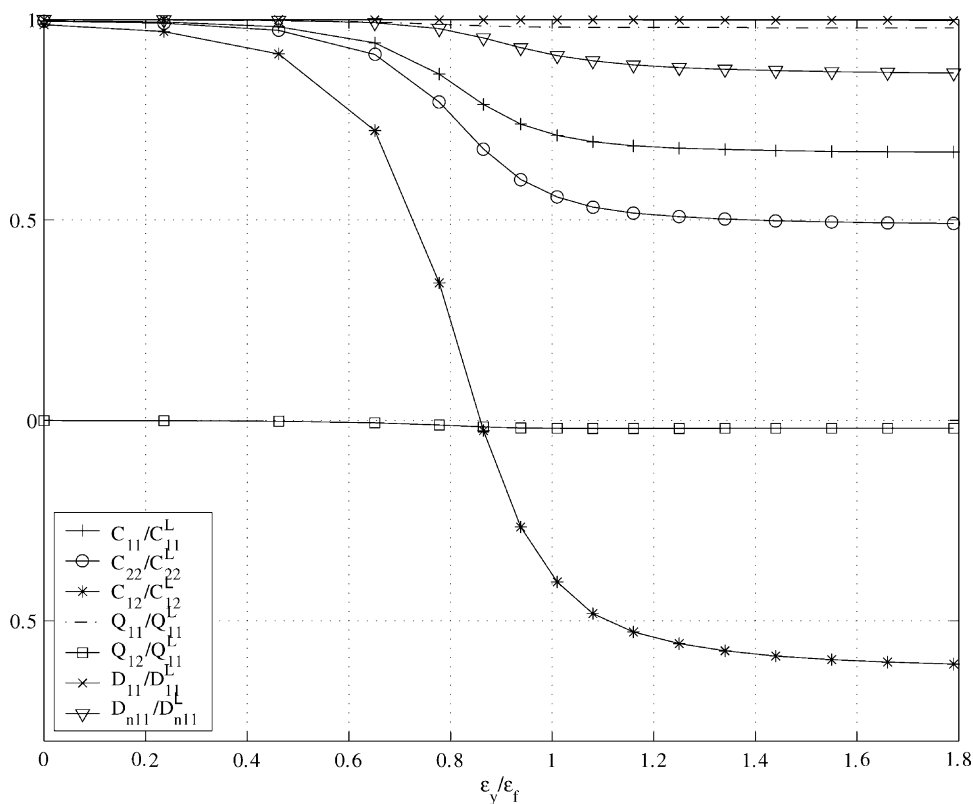


Fig. 4. Change in stiffness properties during local buckling due to axial load for steel angle bar.

Table 1  
Dimensions for stiffened steel plate

Stiffener	$a$ (m)	$b$ (m)	$t$ (m)	$h$ (m)	$t_w$ (m)	$b_f$ (m)	$t_f$ (m)	$\sigma_f$ (MPa)
Angle bar	2.73	0.85	0.0165	0.350	0.012	0.100	0.017	355

general trend found for all the stiffeners investigated here. For smaller imperfections the stiffness reduction will be even more sudden, while for larger imperfections there will be a more gradual transition.

#### 4. Global buckling model

For the following derivations, the stiffeners are assumed to be in the longitudinal direction, but transverse stiffening can be analyzed simply by switching panel length and breadth. The stiffened panel is supported on all edges by transverse and longitudinal girders. The length of the panel is  $a$ , while the width is  $B$ . The loads considered are in-plane compression or tension, shear force, and lateral pressure. The edge loads are assumed to be constant in magnitude.

Two stiffener spans and panel widths are included in the model. The intention is to account properly for the effect of lateral pressure on the panel. The pressure must be carried by the stiffeners, and the deflection of the stiffeners may therefore be a combination of the simply supported mode and the clamped mode (Fig. 5). The deflection shape is therefore taken as a combination of sine terms and cosine terms:

$$w = w^s + w^c \quad (35)$$

$$w_0 = w_0^s + w_0^c \quad (36)$$

where  $s$  and  $c$  denote sine and cosine mode deflection, respectively:

$$w^s = \sum_{m=1}^{M_s} \sum_{n=1}^{N_s} A_{mn}^s \sin\left(\frac{m\pi x}{a}\right) \sin\left(\frac{n\pi y}{B}\right) \quad (37)$$

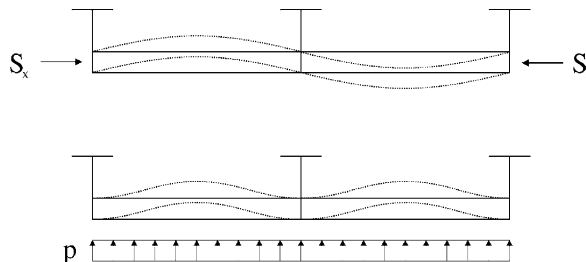


Fig. 5. Global deflection of stiffener in simply supported mode and clamped mode.

$$w^c = \sum_{m=1}^{M_c} \sum_{n=1}^{N_c} \frac{A_{mn}^c}{2} \left[ 1 - \cos\left(\frac{2m\pi x}{a}\right) \right] \sin\left(\frac{n\pi y}{B}\right) \tag{38}$$

$$w_0^s = \sum_{m=1}^{M_s} \sum_{n=1}^{N_s} B_{mn}^s \sin\left(\frac{m\pi x}{a}\right) \sin\left(\frac{n\pi y}{B}\right) \tag{39}$$

$$w_0^c = \sum_{m=1}^{M_c} \sum_{n=1}^{N_c} \frac{B_{mn}^c}{2} \left[ 1 - \cos\left(\frac{2m\pi x}{a}\right) \right] \sin\left(\frac{n\pi y}{B}\right) \tag{40}$$

The anisotropic material law for plane stress, using the stress resultants  $N_1$ ,  $N_2$ , and  $N_3$ , is:

$$\begin{bmatrix} N_1 \\ N_2 \\ N_3 \end{bmatrix} = \begin{bmatrix} C_{11} & C_{12} & C_{13} \\ C_{21} & C_{22} & C_{23} \\ C_{31} & C_{32} & C_{33} \end{bmatrix} \begin{bmatrix} \varepsilon_1 \\ \varepsilon_2 \\ \gamma_3 \end{bmatrix} \tag{41}$$

The corresponding flexibility relation is needed for derivation of the stress function. It is written as:

$$\begin{bmatrix} \varepsilon_1 \\ \varepsilon_2 \\ \gamma_3 \end{bmatrix} = \begin{bmatrix} M_{11} & M_{12} & M_{13} \\ M_{21} & M_{22} & M_{23} \\ M_{31} & M_{32} & M_{33} \end{bmatrix} \begin{bmatrix} N_1 \\ N_2 \\ N_3 \end{bmatrix} \tag{42}$$

The stiffness relation for the resultant bending moments is:

$$\begin{bmatrix} M_1 \\ M_2 \\ M_3 \end{bmatrix} = \begin{bmatrix} D_{11} & D_{12} & D_{13} \\ D_{21} & D_{22} & D_{23} \\ D_{31} & D_{32} & D_{33} \end{bmatrix} \begin{bmatrix} \kappa_1 \\ \kappa_2 \\ \kappa_3 \end{bmatrix} \tag{43}$$

It is assumed that there is no coupling between resultant forces and moments, i.e. all  $Q_{ij}$  terms are zero. This can be done by performing a neutralization of the stiffness coefficients, as explained in [2]. This means that the bending stiffness coefficients are redefined so that no coupling occurs. The neutral bending stiffness matrix  $\bar{\mathbf{D}}$  is calculated from the original stiffness as  $\bar{\mathbf{D}} = \mathbf{D} - \mathbf{Q}^T \mathbf{C}^{-1} \mathbf{Q}$ . For simplicity, the symbol  $\mathbf{D}$  is used in the following to denote the neutral bending stiffness matrix.

Using large deflection plate theory [10], the general requirement for strain compatibility can be written as:

$$\varepsilon_{x,yy} + \varepsilon_{y,xx} - \gamma_{xy,xy} = w_{,xy}^2 - w_{,xx}w_{,yy} + 2w_{0,xy}w_{,xy} - w_{0,yy}w_{,xx} - w_{,yy}w_{0,xx} \tag{44}$$

Following the same approach as was used in [11], a stress function  $F$  is defined in terms of the stress resultants  $N_i$  in the stiffened plate, so that:

$$N_1 = F_{,yy} \tag{45}$$

$$N_2 = F_{,xx} \tag{46}$$

$$N_3 = -F_{,xy} \tag{47}$$

Using the material law as defined above, and introducing the stress function  $F$ , the compatibility equation for the anisotropic plate can be written as:

$$M_{1111}F_{,yyyy} + M_{2222}F_{,xxxx} + (2M_{1122} + M_{1212})F_{,xxyy} - 2M_{1112}F_{,xyyy} - M_{2221}F_{,yxxx} = w_{,xy}^2 + 2w_{0,xy}w_{,xy} - w_{,xx}w_{,yy} - w_{0,yy}w_{,xx} - w_{,yy}w_{0,xx} \quad (48)$$

The solution to this equation is more complex than for an isotropic plate, due to the nonzero coefficients  $M_{1112}$  and  $M_{2221}$ . A solution is found by assuming the stress function to consist of the following terms:

$$F = F_0 + F_{s1} + F_{s2} + F_{c1} + F_{c2} + F_{sc1} + F_{sc2} \quad (49)$$

where

$$F_0 = -\frac{S_x y^2 t}{2} - \frac{S_y x^2 t}{2} - S_{xy} x y t \quad (50)$$

$$F_{s1} = \sum_0^{2M_s} \sum_0^{2N_s} f_{mn}^{s1} \cos\left(\frac{m\pi x}{a}\right) \cos\left(\frac{n\pi y}{B}\right) \quad (51)$$

$$F_{s2} = \sum_0^{2M_s} \sum_0^{2N_s} f_{mn}^{s2} \sin\left(\frac{m\pi x}{a}\right) \sin\left(\frac{n\pi y}{B}\right) \quad (52)$$

$$F_{c1} = \sum_0^{2M_c} \sum_0^{2N_c} f_{mn}^{c1} \cos\left(\frac{2m\pi x}{a}\right) \cos\left(\frac{n\pi y}{B}\right) \quad (53)$$

$$F_{c2} = \sum_0^{2M_c} \sum_0^{2N_c} f_{mn}^{c2} \sin\left(\frac{2m\pi x}{a}\right) \sin\left(\frac{n\pi y}{B}\right) \quad (54)$$

$$F_{sc1} = \sum_0^{M_s+M_c} \sum_0^{N_s+2N_c} f_{mn}^{sc1} \sin\left(\frac{m\pi x}{a}\right) \cos\left(\frac{n\pi y}{B}\right) \quad (55)$$

$$F_{sc2} = \sum_0^{M_s+M_c} \sum_0^{N_s+2N_c} f_{mn}^{sc2} \cos\left(\frac{m\pi x}{a}\right) \sin\left(\frac{n\pi y}{B}\right) \quad (56)$$

By substitution of the assumed stress function into the compatibility equation, it is found that the coefficients  $f_{mn}^1$  and  $f_{mn}^2$  must be:

$$f_{mn}^{s1} = \frac{1}{4a^2 B^2 (K1s - K2s^2 / K1s)} \sum_{rspq} b_{rspq}^s \left( A_{rs}^s A_{pq}^s + A_{rs}^s B_{pq}^s + A_{pq}^s B_{rs}^s \right) \tag{57}$$

$$f_{mn}^{s2} = -\frac{K2s}{K1s} f_{mn}^{s1} \tag{58}$$

$$f_{mn}^{c1} = \frac{1}{4a^2 B^2 (K1c - K2c^2 / K1c)} \sum_{rspq} b_{rspq}^c \left( A_{rs}^c A_{pq}^c + A_{rs}^c B_{pq}^c + A_{pq}^c B_{rs}^c \right) \tag{59}$$

$$f_{mn}^{c2} = -\frac{K2c}{K1c} f_{mn}^{c1} \tag{60}$$

$$f_{mn}^{sc1} = \frac{1}{4a^2 B^2 (K1sc - K2sc^2 / K1sc)} \sum_{rspq} b_{rspq}^{sc} \left( A_{rs}^s A_{pq}^c + A_{rs}^s B_{pq}^c + A_{pq}^c B_{rs}^s \right) \tag{61}$$

$$f_{mn}^{sc2} = -\frac{K2sc}{K1sc} f_{mn}^{sc1} \tag{62}$$

where

$$K1s = \frac{m^4}{a^4} M_{2222} + \frac{m^2 n^2}{a^2 B^2} (2M_{1122} + M_{1212}) + \frac{n^4}{B^4} M_{1111} \tag{63}$$

$$K2s = 2 \frac{m^3 n}{a^3 B} M_{2221} + 2 \frac{mn^3}{aB^3} M_{1112} \tag{64}$$

$$K1c = 16 \frac{m^4}{a^4} M_{2222} + 4 \frac{m^2 n^2}{a^2 B^2} (2M_{1122} + M_{1212}) + \frac{n^4}{B^4} M_{1111} \tag{65}$$

$$K2c = 16 \frac{m^3 n}{a^3 B} M_{2221} + 4 \frac{mn^3}{aB^3} M_{1112} \tag{66}$$

$$K1sc = \frac{m^4}{a^4} M_{2222} + \frac{m^2 n^2}{a^2 B^2} (2M_{1122} + M_{1212}) + \frac{n^4}{B^4} M_{1111} \tag{67}$$

$$K2sc = -2 \frac{m^3 n}{a^3 B} M_{2221} - 2 \frac{mn^3}{aB^3} M_{1112} \tag{68}$$

and  $f_{0,0}$  is defined as zero. The coefficients  $b_{rspq}^s$ ,  $b_{rspq}^c$ , and  $b_{rspq}^{sc}$  can be found in [12].

The potential of internal energy is generally written as

$$U = \frac{1}{2} \int_V \sigma \varepsilon \, dV \tag{69}$$

The strain is first divided into a constant membrane part  $\varepsilon^m$  and a linearly varying bending part  $\varepsilon^b = z\kappa$ . Integration is then performed over the thickness in order to

express the potential energy as a function of stress resultants:

$$U = \frac{1}{2} \int_V \sigma(\varepsilon^m + \varepsilon^b) dV \quad (70)$$

$$= \frac{1}{2} \int_V \sigma \varepsilon^m dV + \frac{1}{2} \int_V z \sigma \kappa dV \quad (71)$$

$$= \frac{1}{2} \int_A N \varepsilon^m dV + \frac{1}{2} \int_V M \kappa dV \quad (72)$$

$$= U_m + U_b \quad (73)$$

By substitution of the material law, the membrane energy is written as:

$$U_m = \frac{1}{2} \left( M_{11} \int_A N_1^2 dA + M_{22} \int_A N_2^2 dA + M_{33} \int_A N_3^2 dA \right. \\ \left. + 2M_{12} \int_A N_1 N_2 dA + 2M_{13} \int_A N_1 N_3 dA + 2M_{23} \int_A N_2 N_3 dA \right) \quad (74)$$

The membrane energy is calculated by substitution of the stress function and integrating over the plate area. The final expression can be found in [12]. The bending energy is:

$$U_b = \frac{1}{2} \left( D_{11} \int_A \kappa_1^2 dA + D_{22} \int_A \kappa_2^2 dA + D_{33} \int_A \kappa_3^2 dA \right. \\ \left. + 2D_{12} \int_A \kappa_1 \kappa_2 dA + 2D_{13} \int_A \kappa_1 \kappa_3 dA + 2D_{23} \int_A \kappa_2 \kappa_3 dA \right) \quad (75)$$

The resulting expression is found by substituting  $\kappa_1 = w_{,xx}$ ,  $\kappa_2 = w_{,yy}$ , and  $\kappa_3 = 2w_{,xy}$ , and performing the integration. The result is given in [12].

The energy due to in-plane tension or compression load is:

$$T_c = \int_0^{2a} \int_0^{2B} N_1 u_{,x} dy dx + \int_0^{2a} \int_0^{2B} N_2 v_{,y} dy dx \quad (76)$$

The shear energy is:

$$T_\tau = N_3 \int_0^{2a} \int_0^{2B} (u_{,y} + v_{,x}) dy dx \quad (77)$$

The energy due to lateral pressure is:

$$T_{lp} = - \int_0^{2a} \int_0^{2B} p w dy dx \quad (78)$$

It is seen that contribution from the sine deflection to the lateral pressure energy vanishes upon integration. This is due to the anti-symmetry of the sine deflection. Physically, this means that lateral pressure will only give rise to deflection in the

cosine mode. For combined loads, the deflection will be a combination of the two. All final expressions can be found in [12].

## 5. Results

For verification of the computational model developed, analyses were performed using the nonlinear finite element code ABAQUS.

In the first case, the anisotropic material option was applied for the case of an unstiffened plate. This means that all the in-plane stiffness coefficients may be given independently, while the bending stiffness is given directly by integration over the thickness.

Fig. 6 shows the nondimensional load-shortening response for an  $840 \times 980 \times 11$  mm aluminium plate with elastic modulus  $E = 70\,000$  MPa and yield stress  $\sigma_f = 240$  MPa. A combination of lateral pressure  $p = 0.2$  MPa, corresponding to a 20 m water column, and transverse compression,  $S_y = 240$  MPa, is applied proportionally. The combination of in-plane and out-of-plane loads gives a deflection mode in between simply supported and clamped. In order to check the model with anisotropic stiffness, the stiffness was arbitrarily chosen so that  $C_{1112} = C_{2221} = C_{1212}^{\text{iso}}$ . The imperfection is 10 mm in the eigenmode.

It is seen that this load combination results in a snap-back response. The reason is that the imperfection and the transverse loading gives a deflection in the simply supported mode in the first part of the analysis, while the lateral pressure eventually forces the deflection into a clamped mode. It is seen that the agreement between the results from the model and from ABAQUS is very good. This shows that the first order perturbation expansion works very well even for such a complex

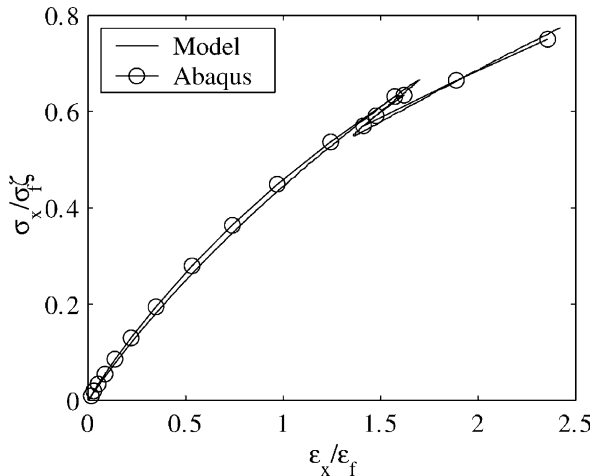


Fig. 6. Load-average strain response for anisotropic plate subjected to combined transverse load and lateral pressure.

Table 2  
Dimensions for aluminium stiffeners

Stiffener	$a$ (m)	$b$ (m)	$t$ (m)	$h$ (m)	$t_w$ (m)	$b_f$ (m)	$t_f$ (m)	$\sigma_f$ (MPa)
Tee bar	2.4	0.32	0.005	0.075	0.005	0.040	0.005	240

response. Also, the lateral pressure effect, which gives a resulting deflection mode in between simply supported and clamped, is well taken care of.

In order to check the bending stiffness formulations, analyses are performed using a stiffened panel in ABAQUS. It is desirable to compare the model with a stiffened panel deflecting in a pure global mode, i.e. without local buckling of plate and stiffeners. One way to achieve this is to model a panel with very large plate thickness compared to the panel dimensions. Such a panel is likely to deflect globally without local deformations.

A stiffened panel consisting of three aluminium profiles (Table 2) is modelled in ABAQUS. The thickness of the plate, the web, and the flange is increased from the original dimensions given in the table to 50 mm. This geometry is so stocky that the resulting deformation is purely in the global mode. Analyses are performed on the stiffened panel in ABAQUS for axial and transverse loading, with an imperfection in the global mode equal to 3.6 mm. Analyses are then performed with the global buckling model using linear anisotropic stiffness coefficients according to the stiffener dimensions, as explained previously. The results are shown in Fig. 7. It is seen that the agreement is very good.

In Fig. 8, the response of this panel under axial loading, calculated using linear stiffness coefficients, is compared with the response calculated using reduced stiffness resulting from local buckling analysis. The imperfection is 3.2 mm in the local mode and 3.6 mm in the global mode. It is seen that the global deflection is larger when the reduced stiffness is applied, as expected. In this analysis, the stiffness

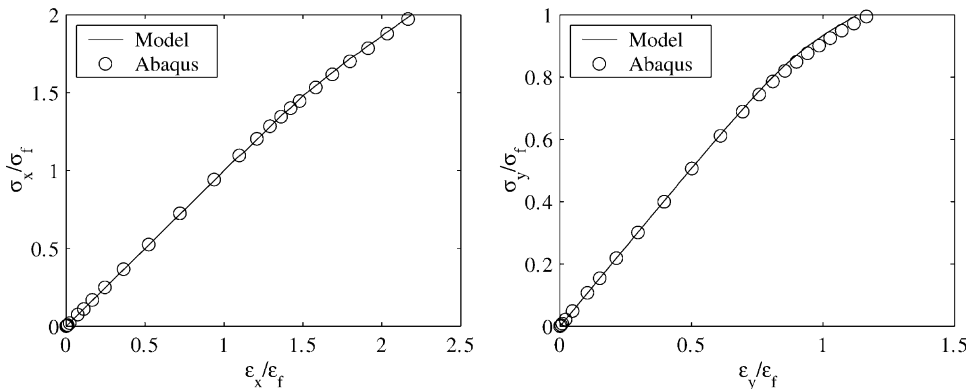


Fig. 7. Load-average strain response due to pure global buckling for stiffened panel subjected to axial compression (left) and transverse compression (right).

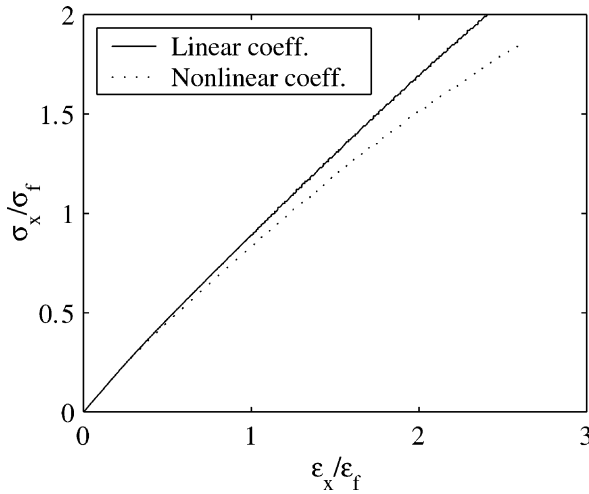


Fig. 8. Load-average strain response during axial load calculated from global buckling model using linear and nonlinear stiffness coefficients.

coefficients input to the global model are gradually reduced, corresponding to the current load factor.

## 6. Concluding remarks

A computational model for the analysis of global buckling and postbuckling of stiffened panels has been derived. The model was developed as part of a tool for buckling assessment of stiffened panels. It is formulated using large deflection plate theory and energy principles. Any combination of biaxial in-plane compression or tension, shear, and lateral pressure may be analyzed. The procedure is semi-analytical in the sense that all energy formulations are derived analytically, while a numerical method is used for solving the resulting set of equations, and for incrementing the solution. The load–deflection curves produced by the proposed model are compared with results from nonlinear FEM. Good correspondence is achieved, and the efficiency of the calculations is high.

The global model is combined with a local buckling model in the DNV computer code PULS [13]. In this program, the ultimate strength of panels is estimated by checking the stress at certain critical points at each increment. Using the von Mises yield criterion, the onset of yielding is taken as the collapse load for design purposes. This is conservative, and a sound, design approach, since yielding will give unwanted permanent deformations in the structure.

## Acknowledgements

This study has been performed with support from the Norwegian Research Council and Det Norske Veritas.

## References

- [1] Byklum E, Amdahl J. A simplified method for elastic large deflection analysis of plates and stiffened panels due to local buckling. *Thin-Walled Structures* 2002;40(11):923–51.
- [2] Det Norske Veritas. PULS 1.5 theory manual. 2003.
- [3] Byklum E, Amdahl J. Nonlinear buckling analysis and ultimate strength prediction of stiffened steel and aluminium panels. The Second International Conference on Advances in Structural Engineering and Mechanics, Pusan. 2002.
- [4] Huseyin K. Nonlinear theory of elastic stability. Leyden: Nordhoff International Publishing; 1975.
- [5] Steen E. Application of the perturbation method to plate buckling problems. Research report in mechanics 98-1, University of Oslo, 1998.
- [6] Ueda Y, Rashed S, Paik J. An incremental Galerkin method for plates and stiffened plates. *Computers and Structures* 1987;27(1):147–56.
- [7] Paik J, Thayamballi A, Lee S, Kang S. A semi-analytical method for the elastic–plastic large deflection analysis of welded steel or aluminium plating under combined in-plane and lateral pressure loads. *Thin-Walled Structures* 2001;39:125–52.
- [8] Steen E. Elastic buckling and postbuckling of eccentrically stiffened plates. *International Journal of Solids and Structures* 1989;25(7):751–68.
- [9] Steen E. Buckling of stiffened plates using a Shanley model approach. Research report in mechanics 99-1, University of Oslo, 1999.
- [10] Marguerre K. Die mittragende Breite der gedruckten Platte. *Luftfahrtforschung* 1937;14(3):121–8.
- [11] Levy S. Bending of rectangular plates with large deflection. Report 737, NACA, 1942.
- [12] Byklum E. Ultimate strength analysis of stiffened steel and aluminium panels using semi-analytical methods. PhD thesis, Norwegian University of Science and Technology, 2002.
- [13] Det Norske Veritas. PULS 1.5 user's manual. 2003.